PROTEINS
STRUCTURE ■ FUNCTION ■ BIOINFORMATICS

On the orientation of the catalytic dyad in aspartic proteases

Ran Friedman* and Amedeo Caflisch*

Department of Biochemistry, University of Zürich, Winterthurerstrasse 190, CH-8057 Zürich, Switzerland

ABSTRACT

The recent re-refinement of the X-ray structure of apo plasmepsin II from *Plasmodium falciparum* suggests that the two carboxylate groups in the catalytic dyad are noncoplanar, (Robbins et al., Acta Crystallogr D Biol Crystallogr 2009;65: 294–296) in remarkable contrast with the vast majority of structures of aspartic proteases. Here, evidence for the noncoplanarity of the catalytic aspartates is provided by analysis of multiple explicit water molecular dynamics (MD) simulations of plasmepsin II, human β-secretase, and HIV-protease. In the MD runs of plasmepsin II, the angle between the planes of the two carboxylates of the catalytic dyad is almost always in the range 60°–120°, in agreement with the perpendicular orientation in the re-refined X-ray structure. The noncoplanar arrangement is prevalent also in the β-secretase simulations, as well as in the runs with the inhibitor-bound proteases. Quantum-mechanics calculations provide further evidence that before catalysis the noncoplanar arrangement is favored energetically in eukaryotic aspartic proteases. Remarkably, the coplanar orientation of the catalytic dyad is observed in MD simulations of HIV-protease at 100 K but not at 300 K, which indicates that the noncoplanar arrangement is favored by conformational entropy. This finding suggests that the coplanar orientation in the crystal structures of apo aspartic proteases is promoted by the very low temperature used for data collection (usually around 100 K).

Proteins 2010; 00:000–000.
© 2009 Wiley-Liss, Inc.

Key words: plasmepsin; beta-secretase; molecular dynamics; density functional theory; hiv protease; scc-dftb; m06.

INTRODUCTION

Aspartic proteases (EC 3.4.23) are a widely distributed group of protein degrading enzymes whose catalytic apparatus consists of two aspartate side chains. Several members of this class of enzymes are relevant therapeutic targets, including the aspartic protease of the human immunodeficiency virus (HIV), plasmepsins in plasmodia (malaria), and human proteases such as renin (hypertension) and β-secretase (Alzheimer's disease). Their three-dimensional structure has been widely studied, and over 600 X-ray structures have been deposited in the protein data bank (PDB[1]). The eukaryotic aspartic proteases share the same native topology. They are comprised of a single polypeptide chain that folds in two homologous domains. The catalytic site is formed at a cleft between the two domains and consists of two aspartates with coplanar arrangement of the two carboxylate groups in almost all PDB structures of aspartic proteases.

Recently, a re-refinement of the crystal structure of apo plasmepsin II (abbreviated as plasmepsin hereafter) has led to the surprising observation that the carboxylate plane of Asp214 is rotated by 66° with respect to the original structure[2] (PDB code 3f9q), breaking the coplanar configuration of the catalytic residues. The orientation of Asp214 in the original structure (1lf4) is the same as in other aspartic proteases.

We have previously run molecular dynamics (MD) simulations of plasmepsin to analyze the hydrogen-bonding network and protonation state of the catalytic dyad,[3] study its activation mechanism,[4] and suggest binding modes of small-molecule inhibitors.[5] Here, the MD data are analyzed to investigate the configuration of the two catalytic aspartates and in particular the relative orientation of their carboxylate groups. It is shown that multiple orientations and positions of the carboxylate groups are possible. Moreover, analysis of MD simulations of human β-secretase[6] and HIV-protease reveals that the plasticity of the catalytic dyad and noncoplanarity of the carboxylate groups are evident in aspartic proteases involved in distinct biological processes in different organisms. Quantum-mechanics (QM) calculations of a model of the catalytic site show that the noncoplanar arrangement is energetically favored in eukaryotic aspartic proteases, while both arrangements are equi-energetic in the retroviral protease. Finally, in MD simulations of HIV-protease, the orientation of the catalytic

Grant sponsor: Forschungskredit University of Zürich.
*Correspondence to: Ran Friedman or Amedeo Caflisch, Department of Biochemistry, University of Zürich, Winterthurerstrasse 190, CH-8057 Zürich, Switzerland.
E-mail: r.friedman@bioc.uzh.ch or caflisch@bioc.uzh.ch.
Received 29 June 2009; Revised 12 November 2009; Accepted 7 December 2009
Published online 21 December 2009 in Wiley InterScience (www.interscience.wiley.com).
DOI: 10.1002/prot.22674

dyad is observed to depend on the temperature: the arrangement is mainly noncoplanar at 300 K and 200 K, and coplanar at 100 K, even in a 100 K simulation started from a 300 K snapshot with almost perpendicular arrangement.

METHODS

Classical MD simulations with explicit solvent

Plasmepsin

The MD simulations of plasmepsin performed with the Gromacs program[7] and the OPLS force field[8] were available from a previous study which showed that Asp214 is protonated.[3] The X-ray structure of uncomplexed plasmepsin (PDB code 1lf4[9]) and the structure of plasmepsin bound to the transition state analogue rs370 (PDB code 1lf2[10]) were used as starting structures. The total simulation times were 40 and 60 ns for the apo and holo structures, respectively. An additional simulation at T = 100 K was run for 41 ns using an identical setup (Table I).

β-Secretase

The MD simulations of β-secretase were available from a previous work.[6] The analysis reported here is carried out on 65 ns of simulations starting from two different structures of apo β-secretase (PDB codes 1sgz[11] and 1w50,[12]), and 30 ns of β-secretase in the complex with a peptidic inhibitor (PDB code 1fkn[13]). All β-secretase runs were performed with protonated Asp32. The β-secretase simulations were carried out with CHARMM[14,15] and the CHARMM22 force field.[16] Analysis of simulations was performed with Gromacs. CHARMM trajectory files were converted into Gromacs trajectories with the computer program Wordom[17] for further analysis.

HIV-protease

The X-ray structure of uncomplexed HIV-protease (PDB code 2pc0,[18]) was used as a starting structure for the MD simulations of HIV-protease. The protein was simulated at temperatures of 100 K, 200 K, and 300 K, where the temperature was kept constant using the velocity rescaling thermostat,[19] and the pressure was coupled to a weak bath.[20] Hydrogens were converted into virtual sites,[21] allowing a timestep of 4 fs. The settings were otherwise identical to Ref. 3. Two runs were carried out at each temperature, where a single catalytic aspartic acid was protonated either at $O_{\delta2}$ (the external oxygen) or at $O_{\delta1}$. Additionally, one simulation at 100 K was started from a snapshot sampled at 300 K with catalytic dyad dihedral angle of 78°, i.e., almost perpendicular orientation. The total simulation time for HIV-protease was 580 ns, and individual runs were carried out for 62–100 ns (Table I).

QM-based geometry optimizations in vacuo

Geometry optimizations were carried out using density functional theory (DFT) for the atoms close to the catalytic dyad (called model hereafter) of eukaryotic and retroviral aspartic proteases. Two models with different number of atoms and different level of theory were used.

The first model included consensus residues Asp-Thr-Gly-Ser/Asp-Ser-Gly-Thr for eukaryotic and Asp-Thr-Gly-Ala for retroviral catalytic sites, and the catalytic water molecule. These models were based on the X-ray structures of plasmepsin bound to pepstatin (PDB code 1xe5) and HIV-protease bound to a transition state inhibitor (PDB code 2uy0[22]). Noninteracting N and C ter-

Table I
Details of MD Simulations

Simulation	Starting structure	Protonated Asp[a]	Length (ns)	Temp. (K)	Catal. dyad dihedral	Force field	Ref.
Plasmepsin							
apo	1lf4	Asp214[b]	40	300	90 ± 27	OPLS	3
inhibitor-bound	1lf2	Asp214[b]	60	300	75 ± 20	OPLS	3
apo	1lf4	Asp214, ext. O	41	100	33 ± 7	OPLS	this work
β-secretase							
apo	1sgz & 1w50	Asp32[b]	65	300	90 ± 33	CHARMM22	6
inhibitor-bound	1fkn	Asp32[b]	30	300	72 ± 19	CHARMM22	6
HIV-protease							
T300	2pc0	[b]	200	300	68 ± 18	OPLS	this work
T200e	2pc0	ext. O	81	200	67 ± 18	OPLS	this work
T200i	2pc0	int. O	62	200	66 ± 13	OPLS	this work
T100e	2pc0	ext. O	94	100	16 ± 7	OPLS	this work
T100i1	2pc0	int. O	72	100	39 ± 8	OPLS	this work
T100i2[c]	T300	int. O	72	100	33 ± 9	OPLS	this work

[a]All MD runs were performed with one of the two catalytic Asp protonated. The residue number is not listed for HIV-protease because of its C_2 symmetry.
[b]At 300 K, the initial position of the hydrogen atom is irrelevant because of the many fast transitions.
[c]The initial conformation of T100i2 is the coordinate set saved after 1 ns of equilibration at 300 K (starting from 2pc0), in which the orientation of the carboxylate groups of the catalytic dyad is noncoplanar (dihedral angle of 78°).

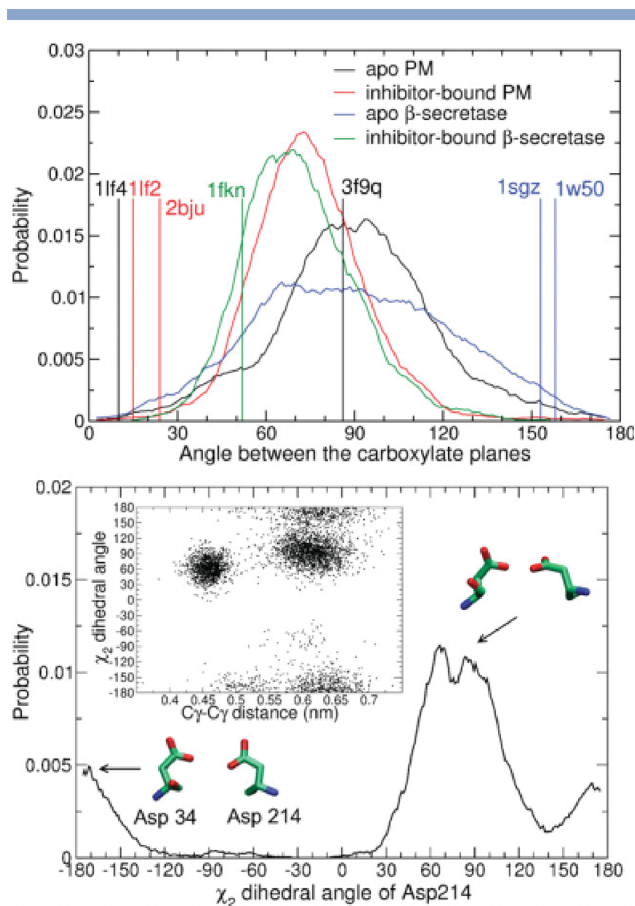

Figure 1

Orientation of the catalytic dyad in the 300 K MD simulations of apo plasmepsin (black), inhibitor-bound plasmepsin (red), apo β-secretase (blue), and inhibitor-bound β-secretase (green). (Top) Distribution of the angle between the planes of the carboxylates of the catalytic dyad from MD simulations. Values for individual X-ray structures are shown by vertical lines with the corresponding PDB code on the top. The coplanar arrangement corresponds to values of the angle smaller than about 30° or larger than 150° as observed for the vast majority of X-ray structures. Note that 3f9q is the recently re-refined X-ray structure of uncomplexed plasmepsin.[2] (Bottom) Distribution of the dihedral angle χ_2 of Asp214 from the MD simulations of uncomplexed plasmepsin. The inset shows a scatter plot of the χ_2 of Asp214 as a function of the separation of the carboxylate groups measured by the Asp34 C_γ– Asp214 C_γ distance.

minal atoms (nitrogen and carbonyl carbon and oxygen that are connected to the downstream or upstream amino acid by a peptide bond) were neglected, resulting in 88 and 86 atoms for the eukaryotic and retroviral systems, respectively. Each system was optimized in the coplanar and noncoplanar arrangements. The calculations were carried out using self consistent charge density functional tight binding (SCC-DFTB[23]), with the computer program DFTB+.[24] Slater-Koster parameters developed by Elstner et al.[23] were used. It has been reported that SCC-DFTB calculations with these parameters are in agreement with DFT calculations using medium-size basis sets,[25,26] although they are orders of magnitude faster. Stereo figures of the optimized models were prepared using the computer program VMD.[27]

In addition to the SCC-DFTB calculations, a more accurate but computationally more expensive level of theory was used for geometry optimization. The model system consisted of the plasmepsin binding site and a peptide group representing a substrate (36 atoms), and optimization was carried out with the M06 multipurpose functional[28] and the 6-31G+** basis set. The initial coordinates were taken from an X-ray structure with pepstatin (PDB code 1xe5). The catalytic residues were modeled as acetic acid (Asp214) and acetate ion (Asp34). The substrate was modeled as CH_3—NH=CO—CH_3, and the catalytic water was included in the system. To prevent distortion due to the small size of the system, the carbon atoms of the catalytic aspartates and the nitrogen atom of the substrate were fixed to the crystallographic positions as in plasmepsin (PDB: 1xe5). As geometry optimization yielded a noncoplanar arrangement of the carboxylate planes of the dyad, a second optimization was performed with carboxylate oxygens fixed in the coplanar orientation for calculating the energy difference with the noncoplanar arrangement. The M06/6-31G+** calculations were performed with the computer program GAMESS.[29]

RESULTS AND DISCUSSION

Plasmepsin

The noncoplanarity of the catalytic dyad (Asp34 and Asp214 in plasmepsin) is evident in the distribution of the angle between the planes of the two catalytic carbox-

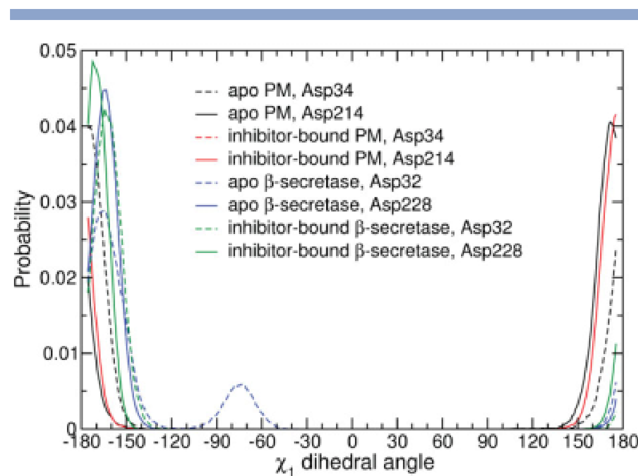

Figure 2

Probability distributions of the χ_1 dihedral angle of the catalytic aspartates. The distributions are shown for the MD simulations of plasmepsin[3] and β-secretase.[6] HIV-protease has essentially identical distributions at all temperatures (not shown). [Color figure can be viewed in the online issue, which is available at www.interscience.wiley.com.]

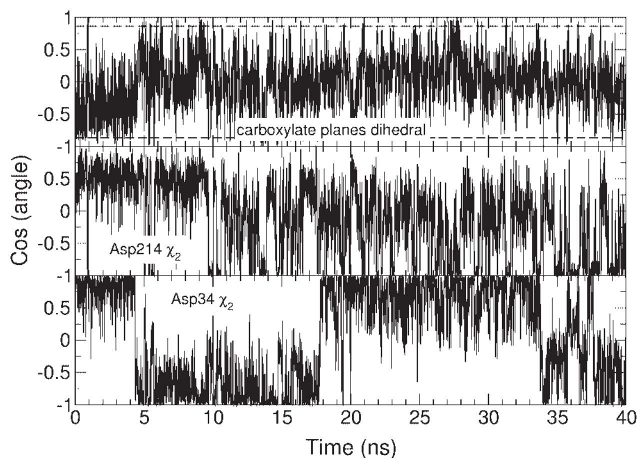

Figure 3

Transitions between rotamers of the catalytic dyad in apo plasmepsin. Time series of the cosine of the angle between the carboxylate planes of the catalytic dyad (top) and the χ_2 dihedral angle of Asp214 (middle) and Asp34 (bottom) calculated along the 300 K MD run of apo plasmepsin. The dihedral angle between the planes changes in the ps to ns time scale. The fluctuations are mainly due to rotations of the χ_2 dihedral of the protonated Asp214, whereas the χ_2 dihedral of Asp34 varies more slowly due to a stable hydrogen bond between Ser37 and the charged carboxylate.

ylates which shows a peak close to 90° and small probability for the coplanar arrangement (Fig. 1). This simulation result is in accord with the newly refined structure.[2] Although the simulations were initiated with the coplanar structure, a noncoplanar arrangement is observed after the equilibration period. Furthermore, the peak is broader for the simulations of uncomplexed plasmepsin (black) than those of the holo plasmepsin (red) because the inhibitor, and in particular its hydroxyl group, restricts the flexibility of the dyad. As the backbone atoms undergo very small displacements during the MD simulations, the spatial orientation of the carboxylate dyad reflects the values of the side chain rotamers of the catalytic aspartates (Asp34 and Asp214 in plasmepsin). Moreover, the χ_1 angle of both Asp34 and Asp214 is always in the trans state (Fig. 2), so that the carboxylate dyad angle is determined solely by the χ_2 (C_α-C_β-C_γ-$O_{\delta 2}$) dihedral angle. The separation of the two carboxylate groups, as measured by the C_γ–C_γ distance, shows a distribution peaked at about 0.45 nm and a broader maximum at about 0.60–0.65 nm (inset of Fig. 1, bottom). The smaller separation corresponds to the direct hydrogen bond and Asp214 χ_2 value of about 30°–90°. On the other hand, the 0.60–0.65 nm distance reflects a water-bridged hydrogen bond which allows for a broader range of χ_2 values of Asp214 (45°–180°).

The time series of the carboxylate dyad angle reveals that rotations between coplanar and noncoplanar orientations occur in the ps to ns time scale (Fig. 3) indicating that there is no significant energy barrier at 300 K. Moreover, the relative orientation of the planes of the two carboxylates is determined by the rotations of both Asp34 and Asp214, with the latter showing a larger amount of transient, that is, 10–100 ps, fluctuations. Despite this rotational flexibility, the hydrogen bond network connecting the catalytic dyad to the flap region (Thr217-Asp214-water1-Asp34-Ser37-Tyr77-Trp41) is preserved along the MD simulations of plasmepsin with protonated Asp214 (see Table II and Fig. 2 in Ref. 3). Note that, in contrast to the 300 K simulations, the catalytic dyad is essentially planar (dihedral angle of 33 ± 7, Table I) in the MD run carried out at 100 K, which is the temperature of X-ray data collection.

β-Secretase

The MD simulations of β-secretase[6] were carried out with a different force field and computer program (see "Methods"), yet the broad distribution of the carboxylate dyad angle in β-secretase (Fig. 1, top) and the fluctuations of the angle are very similar to those observed in the plasmepsin simulations. Interestingly, the orientation of inhibitor-bound β-secretase deviates from planarity in the crystal structure (PDB: 1fkn), and the noncoplanar arrangement was observed also during MD simulations carried out by Cascella et al.[30]

HIV-protease

The MD simulations of HIV-protease show that the dyad is close to coplanar at 100 K, but not at temperatures of 200 K and 300 K. The peak of the distribution of the dihedral angle between the carboxylate planes shifts from coplanar to noncoplanar at temperature higher than 100 K (Fig. 4). Apparently, the rigid coplanar

Table II

Comparison between X-ray Structures and QM-Optimized Models (SCC-DFTB) of the Catalytic Site

		Interatomic distance (Å)[a]		
		QM-optimized		
Atom 1	Atom 2	Noncoplanar	Coplanar	X-ray structure
Eukaryotic protease (plasmepsin)				
Asp34:O_δ	Asp214:O_δ	3.9	3.2	3.5
Asp34:O_δ	Water:O	2.7	2.8	2.8
Asp214:O_δ	Water:O	2.5	2.7	2.8
Asp34:O_δ	Ser37:O_γ	2.8	2.8	2.7
Asp34:O_δ	Ser215:O_γ	2.7	2.7	4.6
Asp214:O_δ	Thr35:O_γ	2.7	3.7	3.5
Asp214:O_δ	Thr217:O_γ	3.0	4.7	2.9
Retroviral proteases (HIV-protease)[b]				
Asp25:O_δ	Asp25′:O_δ	3.5	3.2	3.0
Asp25:O_δ	Water:O	2.7	2.7	–
Asp25′:O_δ	Water:O	2.6	2.6	–
Asp25:O_δ	Thr26′:O_γ	4.4	2.7	4.1
Asp25′:O_δ	Thr26:O_γ	5.3	2.8	4.1

[a]The minimal distance is displayed for distances to carboxylate oxygens.
[b]Residue Asp25′ was protonated.

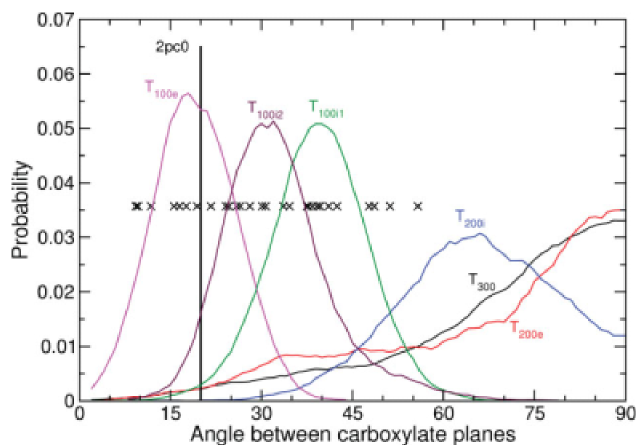

Figure 4

Orientation of the catalytic dyad in the MD simulations of HIV-protease at different temperatures. The colors emphasize the temperatures and initial position of the hydrogen atom. Note that at 300 K the initial position of the proton is irrelevant because of the many fast transitions. The value of the angle (20°) in the X-ray structure used for the simulations (PDB code 2pc0) is shown by a vertical line. The crosses denote the angle in the 28 NMR conformers of HIV-protease in the complex with a cyclic urea inhibitor (PDB code 1bve). The *x*-axis ranges between 0° (exactly coplanar) and 90° (maximally noncoplanar) because of the C_2 symmetry of HIV-protease. [Color figure can be viewed in the online issue, which is available at www.interscience.wiley.com.]

orientation has a lower enthalpy and is preferred at very low temperatures, whereas multiple noncoplanar arrangements are entropically favored and hence preferentially sampled at ambient temperatures (Fig. 5). Interestingly, data collection for the X-ray structures of apo HIV-protease was performed at about 100 K which corroborates the MD results at low temperature.

As the MD simulations suggest a strong temperature dependence and the X-ray structures reflect the very low temperature situation, it is useful to analyze the structures solved by nuclear magnetic resonance (NMR) spectroscopy. There are only five NMR structures of aspartic proteases deposited to the PDB, and they are all of retroviral protease (three HIV and two simian retroviruses). Moreover, in four of these NMR structures the protease is in its monomeric form and thus only one of the two catalytic Asp is present. In the remaining NMR structure, dimeric, that is, catalytically competent, HIV-protease is complexed with a cyclic urea inhibitor (PDB code 1bve[31]). The distribution of the dihedral angle between the carboxylate planes in the 28 NMR conformers (1bve) is close to the one obtained by MD at 100 K (Fig. 4). The almost coplanar arrangement is likely to be a consequence of the presence of the inhibitor, which has two hydroxyl groups pointing toward the carboxylates. Therefore, both carboxylate groups are negatively charged (unlike the monoprotonated state of the apo structure) and their conformational freedom is limited. Moreover, the coplanar conformation may be a consequence of the combined distance geometry algorithm and simulated annealing protocol used to generate the 28 NMR conformers.

QM-based geometry optimizations

To further investigate the relative stability of the planar and coplanar arrangements, QM-based SCC-DFTB geom-

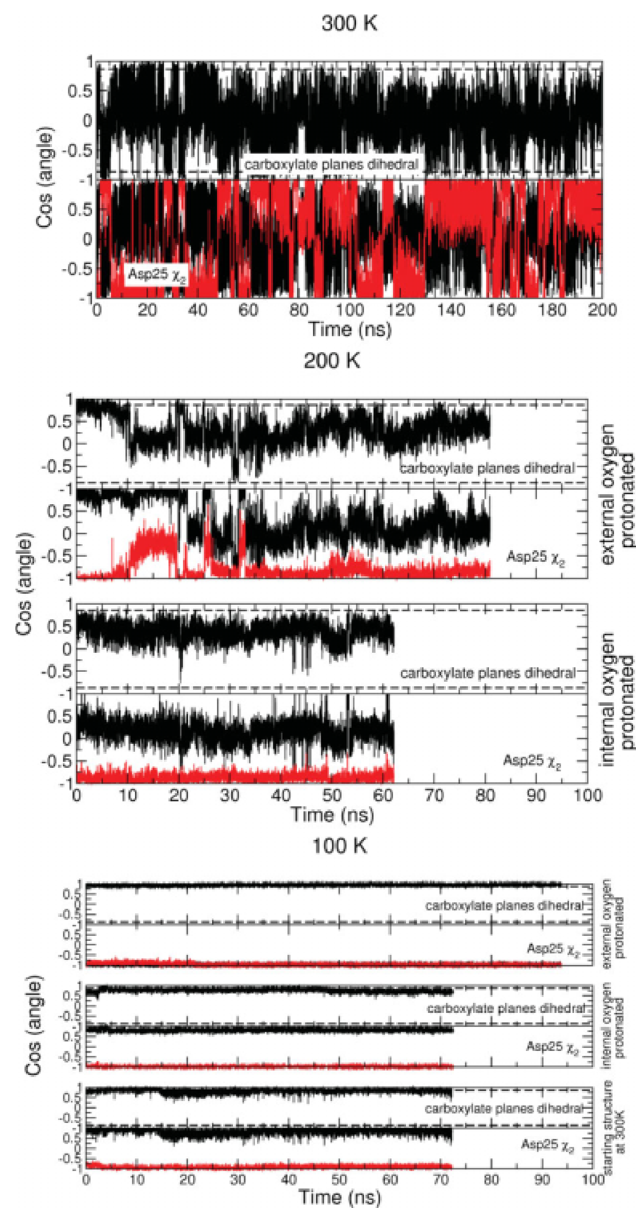

Figure 5

Time series of catalytic dyad dihedral angles in the HIV-protease simulations. The cosines of the dihedral angle between the carboxylate planes of the catalytic dyad and the χ_2 dihedral angles of Asp25 (in black and red for the two monomers) are shown as a function of simulation time. Note that in the run at 100 K started from a snapshot collected at 300 K, the carboxylate planes dihedral changed from 78° to about 25° in the first 0.3 ns of the 1 ns equilibration phase (not shown). [Color figure can be viewed in the online issue, which is available at www.interscience.wiley.com.]

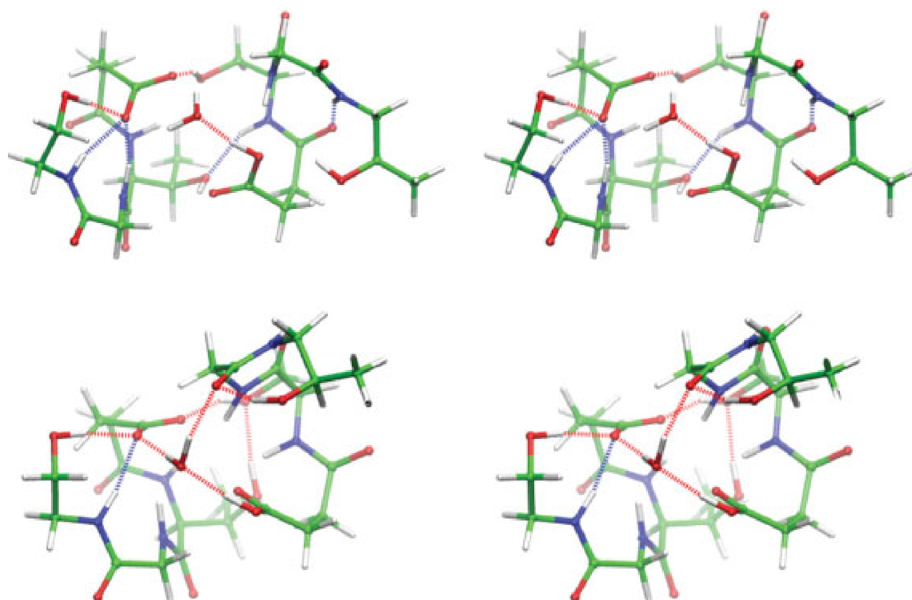

Figure 6

QM-based geometry optimization (SCC-DFTB) of a model of the catalytic site in eukaryotic aspartic proteases (Asp-Thr-Gly-Ser/Asp-Ser-Gly-Thr) shown in stereo. The optimized noncoplanar conformation (top) is more stable than the coplanar (bottom). [Color figure can be viewed in the online issue, which is available at www.interscience.wiley.com.]

etry optimization were carried out using the catalytic dyad and atoms surrounding it for a total of 88 and 86 atoms of plasmepsin and HIV-protease, respectively (see "Methods"). In eukaryotes (Fig. 6), the noncoplanar arrangement (where the angle between the carboxylate planes is about 80°) is energetically favored by 1 kcal/

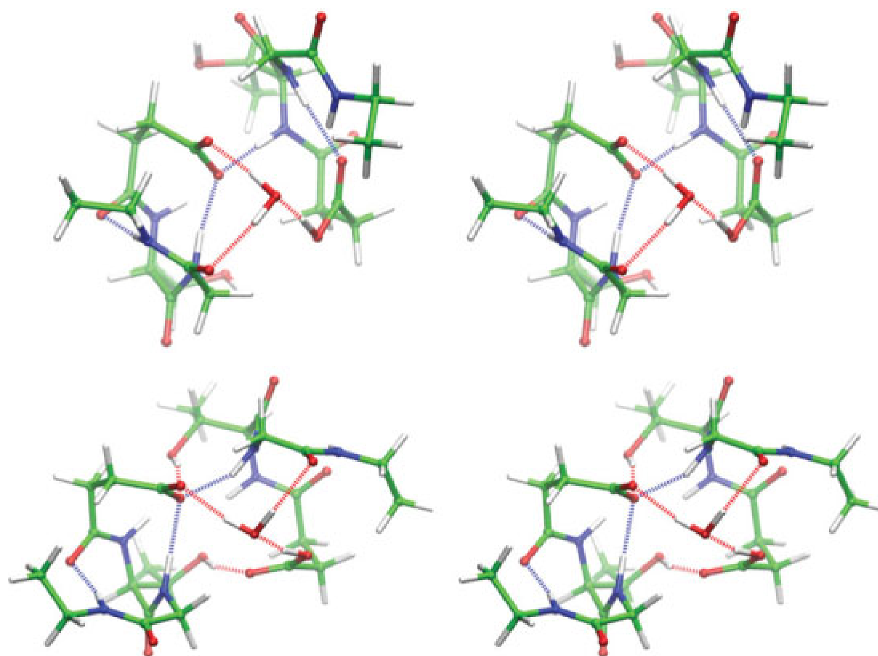

Figure 7

QM-based geometry optimization (SCC-DFTB) of a model of the catalytic site in retroviral aspartic proteases (Asp-Thr-Gly-Ala) shown in stereo. The optimized noncoplanar (top) and planar (bottom) conformations are equally stable. [Color figure can be viewed in the online issue, which is available at www.interscience.wiley.com.]

mol, due to better stabilization of the charged aspartate by the water, and a smaller distance between the hydroxyl moiety of the C-terminal Thr and the carboxylic Asp (Thr217 and Asp214 in plasmepsin, see Table II for atomic distances). In retroviral aspartic proteases (Fig. 7), the two conformations have very similar potential energy (the difference is smaller than 0.1 kcal/mol).

Geometry optimization was carried out also with a more accurate but computationally more expensive theory (DFT with the M06 functional, see "Methods") using a 36 atom model of the eukaryotic catalytic site, including Asp34, Asp214, the catalytic water, and part of the polypeptide substrate. The optimized structure has a noncoplanar arrangement of the dyad, where the angle between the carboxylate planes is 56°. Also, the noncoplanar arrangement is energetically more favorable than the coplanar orientation obtained by optimization with rigid carboxylates. Finally, the deviation from the coplanar orientation is due to rotation of Asp214 in both geometry optimizations of the catalytic site of plasmepsin, that is, in the 88-atom models with SCC-DFTB (Fig. 6) and the 36-atom model with DFT/M06.

CONCLUSIONS

In striking contrast with the abundant structural knowledge on aspartic proteases, a recently published refinement of the crystal structure of uncomplexed plasmepsin suggests that the two carboxylate groups in the catalytic dyad are noncoplanar.[2] Here, we have analyzed explicit water MD simulations of plasmepsin, human β-secretase, and HIV-protease, performed with two different force fields and two different programs for MD simulations. At 300 K, the noncoplanar arrangement is observed not only in MD runs started from the apo structure but also in the simulations of the complex with an inhibitor. Moreover, conformations with multiple relative orientations and variable separations of the carboxylate groups are populated in the simulations. The rotation of the side chains of the catalytic aspartates is a motion in the ps to ns time scale. Despite the plasticity of the binding site, an array of hydrogen bonds involving the binding site residues and structural waters is maintained in the simulations,[3,6] and in the crystal structures of pepsin-like aspartic proteases.[32] This hydrogen-bond array keeps the catalytic aspartates at close proximity,[3] while allowing some flexibility of the binding site. Together with motions of the flap region, which covers the catalytic site,[6,33] this plasticity may enable substrate binding and/or product release. Furthermore, the noncoplanar arrangement may be necessary for initiating the catalytic mechanism, before the formation of the tetrahedral intermediate, as suggested based on crystallographic studies and MD simulations of HIV protease,[34] and QM/MM simulations of β-secretase.[30]

A remarkable temperature dependence of the relative orientation of the two carboxylate groups in the catalytic dyad is observed in MD simulations of apo plasmepsin and HIV-protease. At 300 K, there are frequent rotations (of the χ_2 angle of the two catalytic Asp residues) and mainly noncoplanar arrangement of the two carboxylates, whereas a mainly rigid and coplanar orientation is observed at 100 K (Figs. 4 and 5). Taken together, the simulation results indicate that the discrepancy between coplanar orientation in the X-ray structures (where data are usually collected at 100 K) and noncoplanar arrangement in the MD simulations (at room temperature) is due to conformational entropy effects.

ACKNOWLEDGMENTS

The authors thank an anonymous reviewer for pointing our attention to the difference between eukaryotic and retroviral aspartic proteases in the segment of the sequence close to the catalytic aspartates. They also thank Dr. Stefan Warmuth for interesting discussions and Prof. A. Abebe Gorfe for the MD trajectories of β-secretase.

REFERENCES

1. Berman HM, Westbrook J, Feng Z, Gilliland G, Bhat TN, Weissig H, Shindyalov IN, Bourne PE. The Protein Data Bank. Nucleic Acids Res 2000;28:235–242.
2. Robbins AH, Dunn BM, Agbandje-McKenna M, McKenna R. Crystallographic evidence for noncoplanar catalytic aspartic acids in plasmepsin II resides in the Protein Data Bank. Acta Crystallogr D Biol Crystallogr 2009;65:294–296.
3. Friedman R, Caflisch A. The protonation state of the catalytic aspartates in plasmepsin II. FEBS Lett 2007;581:4120–4124.
4. Friedman R, Caflisch A. Pepsinogen-like activation intermediate of plasmepsin II revealed by molecular dynamics analysis. Proteins 2008;73:814–827.
5. Friedman R, Caflisch A. Discovery of plasmepsin inhibitors by fragment-based docking and consensus scoring. ChemMedChem 2009;4:1317–1326.
6. Gorfe AA, Caflisch A. Functional plasticity in the substrate binding site of β-secretase. Structure 2005;13:1487–1498.
7. Lindahl E, Hess B, van der Spoel D. Gromacs 3.0: a package for molecular simulation and trajectory analysis. J Mol Mod 2001; 7:306–317.
8. Jorgensen WL, Maxwell DS, Tirado-Rives J. Development and testing of the OPLS all-atom force field on conformational energetics and properties of organic liquids. J Am Chem Soc 1996;118:11225–11236.
9. Asojo OA, Gulnik SV, Afonina E, Yu B, Ellman JA, Haque TS, Silva AM. Novel uncomplexed and complexed structures of plasmepsin II, an aspartic protease from *Plasmodium falciparum*. J Mol Biol 2003;327:173–181.
10. Asojo OA, Afotina A, Gulnik SV, Yu B, Erickson JW, Randad R, Medjahed D, Silva AM. Structures of Ser205 mutant plasmepsin II from *Plasmodium falciparum* at 1.8 angstrom in complex with the inhibitors rs367 and rs370. Acta Crystallogr D Biol Crystallogr 2002;58:2001–2008.
11. Hong L, Tang J. Flap position of free memapsin 2 (beta-secretase), a model for flap opening in aspartic protease catalysis. Biochemistry 2004;43:4689–4695.
12. Patel S, Vuillard L, Cleasby A, Murray CW, Yon J. Apo and inhibitor complex structures of BACE (beta-secretase). J Mol Biol 2004;343:407–416.

13. Hong L, Koelsch G, Lin X, Wu S, Terzyan S, Ghosh AK, Zhang XC, Tang J. Structure of the protease domain of memapsin 2 (beta-secretase) complexed with inhibitor. Science 2000;290:150–153.
14. Brooks BR, Bruccoleri RE, Olafson BD, States DJ, Swaminathan S, Karplus M. CHARMM: a program for macromolecular energy, minimization, and dynamics calculations. J Comput Chem 1983;4: 187–217.
15. Brooks BR, Brooks CL, MacKerell AD, Nilsson L, Roux B, Won Y, Archontis G, Bartels C, Boresch S, Caflisch A, Caves L, Cui Q, Dinner A, Fischer S, Gao J, Hodoscek M, Kuczera K, Lazaridis T, Ma J, Paci E, Pastor RW, Post CB, Schaefer M, Tidor B, Venable RW, Woodcock HL, Wu X, Karplus M. CHARMM: the biomolecular simulation program. J Comput Chem 2009;30:1545–1614.
16. MacKerell AD, Bashford D, Bellott M, Dunbrack RL, Evanseck JD, Field MJ, Fischer S, Gao J, Guo H, Ha S, Joseph-McCarthy D, Kuchnir L, Kuczera K, Lau FTK, Mattos C, Michnick S, Ngo T, Nguyen DT, Prodhom B, Reiher WE, Roux B, Schlenkrich M, Smith JC, Stote R, Straub J, Watanabe M, Wiorkiewicz-Kuczera J, Yin D, Karplus M. All-atom empirical potential for molecular modeling and dynamics studies of proteins. J Phys Chem B 1998;102:3586–3616.
17. Seeber M, Cecchini M, Rao F, Settanni G, Caflisch A. Wordom: a program for efficient analysis of molecular dynamics simulations. Bioinformatics 2007;23:2625–2627.
18. Heaslet H, Rosenfeld R, Giffin M, Lin YC, Tam K, Torbett BE, Elder JH, McRee DE, Stout CD. Conformational flexibility in the flap domains of ligand-free (HIV) protease. Acta Crystallogr D Biol Crystallogr 2007;63:866–875.
19. Bussi G, Donadio D, Parrinello M. Canonical sampling through velocity rescaling. J Chem Phys 2007;126:014101.
20. Berendsen HJC, Postma JPM, DiNola A, Haak JR. Molecular dynamics with coupling to an external bath. J Chem Phys 1984;81:3684–3690.
21. Feenstra KA, Hess B, Berendsen HJC. Improving efficiency of large time-scale molecular dynamics simulations of hydrogen-rich systems. J Comput Chem 1999;20:786–798.
22. Wu X, Ohrngren P, Ekegren JK, Unge J, Unge T, Wallberg H, Samuelsson B, Hallberg A, Larhed M. Two-carbon-elongated HIV-1 protease inhibitors with a tertiary-alcohol-containing transition-state mimic. J Med Chem 2008;51:1053–1057.
23. Elstner M, Porezag D, Jungnickel G, Elsner J, Haugk M, Frauenheim T, Suhai S, Seifert G. Self-consistent-charge density-functional tight-binding method for simulations of complex materials properties. Phys Rev B 1998;58:7260–7268.
24. Aradi B, Hourahine B, Frauenheim T. DFTB+, a sparse matrix-based implementation of the DFTB method. J Phys Chem A 2007;111:5678–5684.
25. Elstner M, Jalkanen KJ, Knapp-Mohammady M, Frauenheim T, Suhai S. Energetics and structure of glycine and alanine based model peptides: approximate SCC-DFTB, AM1 and PM3 methods in comparison with DFT, HF and MP2 calculations. Chem Phys 2001;263:203–219.
26. Friedman R, Fischer S, Nachliel E, Scheiner S, Gutman M. Minimum energy pathways for proton transfer between adjacent sites exposed to water. J Phys Chem B 2007;111:6059–6070.
27. Humphrey W, Dalke A, Schulten K. VMD: visual molecular dynamics. J Mol Graph 1996;14:33–38.
28. Zhao Y, Truhlar DG. The M06 suite of density functionals for main group thermochemistry, thermochemical kinetics, noncovalent interactions, excited states, and transition elements: two new functionals and systematic testing of four M06 functionals and twelve other functionals. Theor Chem Acc 2008;120:215–214.
29. Schmidt MW, Baldridge KK, Boatz JA, Elbert S, Gordon M, Jensen JH, Koseki S, Matsunaga N, Nguyen KA, Su S, Windus TL, Dupuis M, Montgomery JA. General atomic and molecular electronic structure system. J Comput Chem 1993;14:1347–1363.
30. Cascella M, Micheletti C, Rothlisberger U, Carloni P. Evolutionarily conserved functional mechanics across pepsin-like and retroviral aspartic proteases. J Am Chem Soc 2005;127:3734–3742.
31. Yamazaki T, Hinck AP, Wang YX, Nicholson LK, Torchia DA, Wingfield P, Stahl SJ, Kaufman JD, Chang CH, Domaille PJ, Lam PY. Three-dimensional solution structure of the HIV-1 protease complexed with DMP323, a novel cyclic urea-type inhibitor, determined by nuclear magnetic resonance spectroscopy. Protein Sci 1996;5:495–506.
32. Andreeva NS, Rumsh LD. Analysis of crystal structures of aspartic proteinases: on the role of amino acid residues adjacent to the catalytic site of pepsin-like enzymes. Protein Sci 2001;10:2439–2450.
33. Chang CE, Trylska J, Tozzini V, McCammon JA. Binding pathways of ligands to HIV-1 protease: coarse-grained and atomistic simulations. Chem Biol Drug Des 2007;69:5–13.
34. Johnson EC, Malito E, Shen Y, Pentelute B, Rich D, Florián J, Tang WJ, Kent SB. Insights from atomic-resolution X-ray structures of chemically synthesized HIV-1 protease in complex with inhibitors. J Mol Biol 2007;373:573–586.